

## Condensed Phases of Difluoramine and Its Alkali-Metal Fluoride Adducts

Karl O. Christe\* and Richard D. Wilson

Received August 13, 1986

Infrared and Raman spectra of  $\text{HNF}_2$  and  $\text{DNF}_2$  in the liquid and the solid phases show that the compounds are associated through hydrogen bridges between the nitrogen atoms. Raman spectra of the  $\text{KF}$ ,  $\text{RbF}$ , and  $\text{CsF}$  adducts and infrared spectra of the  $\text{RbF}$  adduct of difluoramine are interpreted in terms of strongly hydrogen-bridged  $[\text{F}\cdots\text{HNF}_2]^-$  anions. For the  $\text{CsF}$  and  $\text{RbF}$  adducts evidence was obtained for the existence of a distinct second modification of the  $[\text{F}\cdots\text{HNF}_2]^-$  anion with a significantly stronger hydrogen bridge. The reactions of  $\text{KF}\cdot\text{HNF}_2$  with  $\text{TeF}_5\text{OF}$ ,  $\text{OF}_2$ ,  $\text{FONO}_2$ , and  $\text{FOClO}_3$  were studied and resulted in the fluorination of  $\text{HNF}_2$  to  $\text{HF}$  and  $\text{N}_2\text{F}_4$ .

### Introduction

Although  $\text{HNF}_2$  (difluoramine or fluorimide) has been known<sup>1,2</sup> since 1959, the literature on this interesting compound is sparse. This lack of data may be attributed to the fact that  $\text{HNF}_2$  is a vicious explosive.<sup>3-5</sup> While studying alkali-metal fluoride catalyzed<sup>5-7</sup> reactions of  $\text{HNF}_2$  with various inorganic hypofluorites, we became interested also in the nature of the  $\text{MF}\cdot\text{HNF}_2$  adducts ( $\text{M} = \text{K}, \text{Rb}, \text{Cs}$ ). The existence of these adducts was reported<sup>6</sup> in 1965, and it was shown that  $\text{KF}\cdot\text{HNF}_2$ ,  $\text{RbF}\cdot\text{HNF}_2$ , and  $\text{CsF}\cdot\text{HNF}_2$  are stable up to about  $-90$ ,  $-72$ , and  $-64$  °C, respectively. Whereas  $\text{KF}\cdot\text{HNF}_2$  and  $\text{RbF}\cdot\text{HNF}_2$  undergo smooth dissociation on warm-up,  $\text{CsF}\cdot\text{HNF}_2$  invariably explodes before reaching room temperature.<sup>6</sup> The nature of these adducts has previously been studied by low-temperature infrared spectroscopy, and it was postulated that  $\text{CsF}\cdot\text{HNF}_2$  possesses a structure different from those of the other  $\text{MF}\cdot\text{HNF}_2$  adducts.<sup>8</sup> However, the experimental evidence in support of either structure was not convincing due to strong interference from water and impurity bands. In order to obtain more reliable data on these interesting adducts, we have recorded their low-temperature Raman and infrared spectra. Since for difluoramine only gas-phase<sup>9</sup> and partial, low-resolution, solid-phase<sup>10</sup> infrared spectra had previously been reported, it became also necessary to record its infrared and Raman spectra in the condensed phases. This allowed a better distinction between  $\text{MF}\cdot\text{HNF}_2$  bands and those due to associated  $\text{HNF}_2$  and provided some insight into the nature of the association of  $\text{HNF}_2$  in the condensed phases.

### Experimental Section

**Caution!** Difluoramine is highly explosive,<sup>10,11</sup> and protective shielding and clothing should be used during handling operations. The compound was always condensed at  $-142$  °C, and the use of a  $-196$  °C bath for condensing  $\text{HNF}_2$  should be avoided.<sup>3</sup> Furthermore, the  $\text{CsF}\cdot\text{HNF}_2$  adduct invariably explodes before reaching  $0$  °C.<sup>6</sup> The hypofluorites  $\text{FOClO}_3$ ,<sup>11</sup>  $\text{FONO}_2$ ,<sup>11</sup> and  $\text{TeF}_5\text{OF}$ <sup>12</sup> are also shock sensitive and must be handled with the same precautions.

**Materials and Apparatus.** Difluoramine was handled in either a glass or all Teflon-FEP and Teflon-PFA vacuum line to avoid metal fluoride catalyzed HF elimination. Other volatile materials were handled in a stainless-steel vacuum line equipped with Teflon-FEP U-traps, 316 stainless-steel bellows-seal valves, and a Heise Bourdon tube-type pressure gauge. Nonvolatile materials were handled in the dry  $\text{N}_2$  atmosphere of a glovebox.

Difluoramine was prepared by hydrolysis of difluorourea using a literature method.<sup>3</sup> For the synthesis of  $\text{DNF}_2$ , a previously reported me-

thod involving H-D exchange between  $\text{HNF}_2$  and a large excess of  $\text{D}_2\text{O}^9$  produced only a low yield of  $\text{DNF}_2$ , and the sample still contained 14% of  $\text{HNF}_2$ . Essentially pure  $\text{DNF}_2$  was obtained in high yield by the method used for the preparation of  $\text{HNF}_2$ ,<sup>3</sup> with  $\text{NH}_2\text{CONH}_2$ ,  $\text{H}_2\text{O}$ , and  $\text{H}_2\text{SO}_4$  substituted by their deuteriated analogues. The alkali metal fluorides were dried by fusion in a platinum crucible, followed by immediate transfer of the hot clinkers to the dry  $\text{N}_2$  atmosphere of a glovebox. The  $\text{RbF}$  crystal (Semi-Elements Inc.) used for the low-temperature infrared study of the  $\text{RbF}\cdot\text{HNF}_2$  adduct was freshly cleaved with a razor blade in the drybox and mounted in a dry  $\text{N}_2$  atmosphere into the tip of the helium refrigerator. Small amounts of moisture absorbed onto the surface of the  $\text{RbF}$  crystal were completely removed by pumping on the crystal in the infrared beam for 24 h at  $10^{-6}$  Torr. Literature methods were used for the syntheses of  $\text{FONO}_2$ ,<sup>13</sup>  $\text{TeF}_5\text{OF}$ ,<sup>14</sup> and  $\text{FOClO}_3$ .<sup>15</sup>  $\text{OF}_2$  (Allied Chemical) was purified by fractional condensation at  $-210$  °C prior to its use. The alkali-metal fluoride-difluoramine adducts were generally prepared by condensing an excess of  $\text{HNF}_2$  onto the alkali-metal fluoride at  $-142$  °C, warming the mixture to  $-78$  °C for several hours, and then removing the excess of  $\text{HNF}_2$  in a dynamic vacuum at  $-64$ ,  $-78$ , and  $-95$  °C for  $\text{CsF}\cdot\text{HNF}_2$ ,  $\text{RbF}\cdot\text{HNF}_2$ , and  $\text{KF}\cdot\text{HNF}_2$ , respectively. The composition of the resulting adducts generally approached at 1:1 mole ratio.

Infrared spectra were recorded in the range  $4000$ – $200$   $\text{cm}^{-1}$  on a Perkin-Elmer Model 283 spectrophotometer. The spectra of gases were obtained by using a Teflon cell of 5-cm path length equipped with  $\text{AgCl}$  windows. The low-temperature infrared spectra were obtained at various temperatures with an Air Products Model DE 202S helium refrigerator equipped with internal  $\text{RbF}$  and external  $\text{CsI}$  windows. The Raman spectra were recorded on a Spex Model 1403 spectrophotometer using the 647.1-nm exciting line of a Kr ion laser. Sealed, 3-mm-o.d. quartz tubes were used as sample containers in the transverse-viewing-transverse-excitation mode. For neat  $\text{HNF}_2$  the tip of the tube was drawn out to a smaller diameter to minimize the sample size. A previously described<sup>16</sup> device was used for recording the low-temperature spectra.

**$\text{TeF}_5\text{OF}\cdot\text{KF}\cdot\text{HNF}_2$  System.** A passivated (with  $\text{ClF}_3$ ), 0.5-in.-o.d. Teflon-FEP ampule equipped with a Teflon-PFA valve (Galtek Corp.) was loaded in the drybox with finely powdered, dry  $\text{KF}$  (2.0 g). On the glass vacuum line,  $\text{HNF}_2$  (3.2 mmol) was added to the ampule at  $-142$  °C, and the mixture was kept at  $-78$  °C for 1 h. On the steel-Teflon vacuum line,  $\text{TeF}_5\text{OF}$  (1.57 mmol) was added at  $-196$  °C. The ampule was slowly warmed to  $-78$  °C for 87 h by means of a  $\text{CO}_2$ -liquid- $\text{N}_2$  slush bath and then to  $-64$  °C for 1 h. The material volatile at  $-64$  °C was fractionated through a series of traps kept at  $-78$ ,  $-95$ ,  $-126$ , and  $-196$  °C and consisted of  $\text{N}_2\text{F}_4$  (1.55 mmol) and traces of  $\text{TeF}_6$ ,  $\text{TeF}_5\text{OTeF}_5$ , and  $\text{FNO}$ . Then the ampule was allowed to warm to  $25$  °C, and the volatile material was fractionated through traps kept at  $-78$ ,  $-126$ , and  $-196$  °C. It consisted of  $\text{N}_2\text{F}_4$  (0.05 mmol),  $\text{TeF}_5\text{OH}$  (0.35 mmol), and traces of  $\text{TeF}_6$ ,  $\text{HF}$ , and  $\text{TeF}_5\text{OTeF}_5$ . The vibrational spectra of the white solid residue showed the presence of  $\text{HF}_2^-$  and  $\text{TeF}_5\text{O}^-$ .

**$\text{OF}_2\cdot\text{KF}\cdot\text{HNF}_2$  System.** The  $\text{KF}\cdot\text{HNF}_2$  adduct was prepared as described above from  $\text{KF}$  (7.3 mmol) and  $\text{HNF}_2$  (4.2 mmol), and  $\text{OF}_2$  (2.95 mmol) was added at  $-196$  °C. After slow warm-up to  $-78$  °C no noticeable reaction had occurred. Repeating the reaction at  $-22$  °C for 1 h resulted in a 73% consumption of the  $\text{OF}_2$  and the formation of  $\text{N}_2\text{F}_4$  (1.0 mmol) as the main product.

**$\text{FOClO}_3\cdot\text{KF}\cdot\text{HNF}_2$  System.** A mixture of  $\text{FOClO}_3$  (5.65 mmol) and  $\text{KF}\cdot\text{HNF}_2$  ( $\text{KF}$  69 mmol,  $\text{HNF}_2$  7.44 mmol), when warmed slowly from

- (1) Kennedy, A.; Colburn, C. B. *J. Am. Chem. Soc.* **1959**, *81*, 2906.
- (2) Lawton, E. A.; Weber, J. Q. *J. Am. Chem. Soc.* **1959**, *81*, 4755.
- (3) Lawton, E. A.; Weber, J. Q. *J. Am. Chem. Soc.* **1963**, *85*, 3595.
- (4) Klopotek, D. L.; Hobrock, B. G. *Inorg. Chem.* **1967**, *6*, 1750.
- (5) De Marco, R. A.; Shreeve, J. M. *Inorg. Chem.* **1973**, *12*, 1896.
- (6) Lawton, E. A.; Pilipovich, D.; Wilson, R. D. *Inorg. Chem.* **1965**, *4*, 118.
- (7) Maya, W.; Pilipovich, D.; Warner, M. G.; Wilson, R. D.; Christe, K. O. *Inorg. Chem.* **1983**, *22*, 810.
- (8) Dubb, H. E.; Greenough, R. C.; Curtis, E. C. *Inorg. Chem.* **1965**, *4*, 648.
- (9) Comeford, J. J.; Mann, D. E.; Schoen, L. J.; Lide, D. R., Jr. *J. Chem. Phys.* **1963**, *38*, 461.
- (10) Craig, A. D. *Inorg. Chem.* **1964**, *3*, 1628.
- (11) Lawless, E. W.; Smith, I. C. *Inorganic High Energy Oxidizers*; Marcel Dekker: New York, 1968; p 69.
- (12) Schack, C. J.; Wilson, W. W.; Christe, K. O. *Inorg. Chem.* **1983**, *22*, 18.

- (13) Miller, R. H.; Bernitt, D. L.; Hisatsune, I. C. *Spectrochim. Acta, Part A* **1967**, *23A*, 223.
- (14) Schack, C. J.; Christe, K. O. *Inorg. Chem.* **1984**, *23*, 2922.
- (15) Christe, K. O.; Wilson, W. W. *Inorg. Chem.* **1980**, *19*, 1494.
- (16) Miller, F. A.; Harney, B. M. *Appl. Spectrosc.* **1969**, *23*, 8.

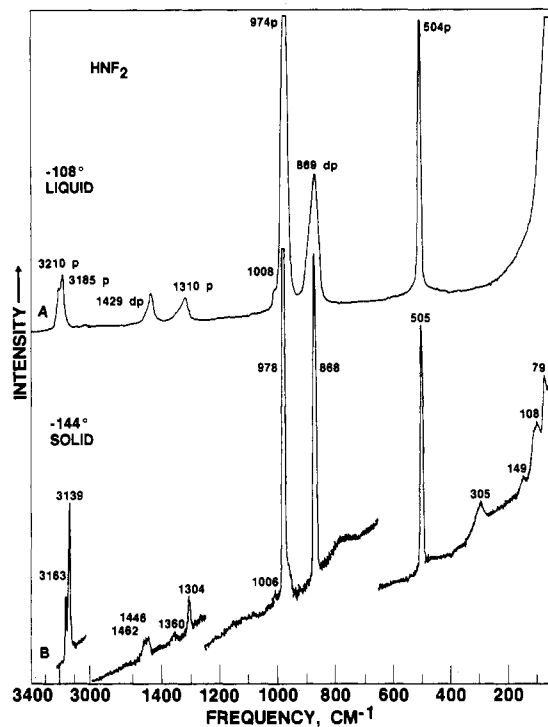


Figure 1. Raman spectra of liquid and solid  $\text{HNF}_2$ .

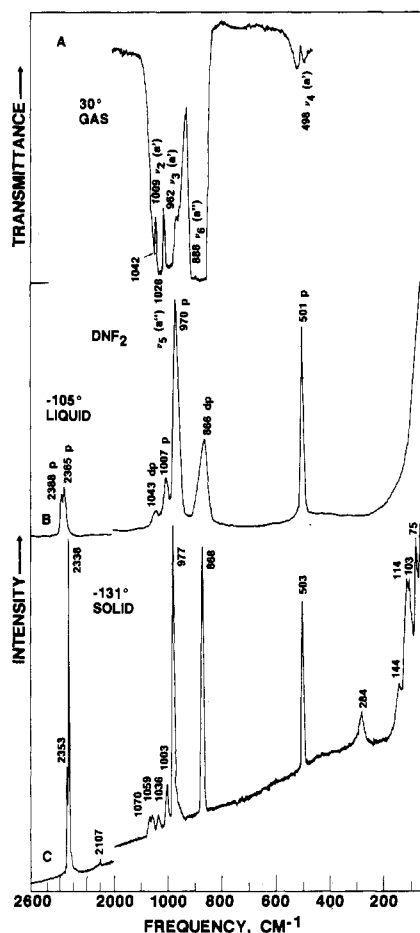


Figure 2. Vibrational spectra of  $\text{DNF}_2$ : trace A, infrared spectrum of the gas at 270 Torr in a 5-cm path length cell; traces B and C, Raman spectra of liquid and solid  $\text{DNF}_2$ , respectively.

-196 to -78 °C resulted in an explosion.

**FONO<sub>2</sub>-KF·HNF<sub>2</sub> System.** A mixture of FONO<sub>2</sub> (0.92 mmol) and KF·HNF<sub>2</sub> (KF 172 mmol, HNF<sub>2</sub> 1.22 mmol), when warmed slowly from -142 to -78 °C and then to +25 °C during fractionation of the volatile

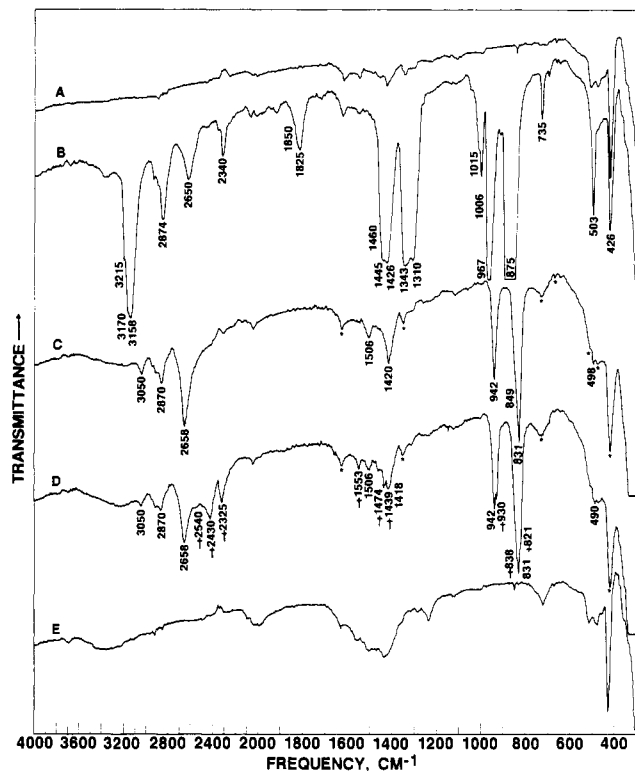


Figure 3. Infrared spectra of solid  $\text{HNF}_2$  and of the  $\text{RbF}\cdot\text{HNF}_2$  adduct at -220 °C: trace A, background of the  $\text{RbF}$  window; trace B, solid  $\text{HNF}_2$ ; trace C,  $\text{RbF}\cdot\text{HNF}_2$  adduct generated by cycling the deposit of trace B through -110 °C, with the bands marked by an asterisk due to cell background; trace D, spectrum produced by cycling deposit of trace C through -105 °C, with the new set of bands marked by a dagger ascribed to the second, more strongly hydrogen-bridged species; trace E, cell background after cycling through 25 °C with pumping.

material, produced  $\text{N}_2\text{F}_4$  (0.5 mmol) with  $\text{NO}_2$ ,  $\text{FNO}_2$ , and some  $\text{O}_2$  as the major volatile byproducts.

## Results and Discussion

**Vibrational Spectra of Difluoramine.** Infrared spectra were recorded for gaseous  $\text{HNF}_2$  and  $\text{DNF}_2$  and solid  $\text{HNF}_2$ . Raman spectra were measured for the liquid and solid phases of  $\text{HNF}_2$  and  $\text{DNF}_2$ . The spectra are given in Figures 1–3, and the observed frequencies and their assignments are summarized in Table I.

The infrared spectrum of gaseous  $\text{HNF}_2$  was in excellent agreement with previous results by Lide and co-workers<sup>9</sup> and requires no further comment. These authors also reported four fundamental vibrations for gaseous  $\text{DNF}_2$ , which were measured on a partially deuterated sample. In our study, for a completely deuterated sample, a fifth fundamental,  $\nu_4(a'')$ , was observed at 498  $\text{cm}^{-1}$ . Furthermore, we prefer to assign the center of the  $\nu_5(a'')$  band to 1028  $\text{cm}^{-1}$  and not to the maximum at 1042  $\text{cm}^{-1}$ , which, we believe, represents the maximum of the R branch of  $\nu_5$  (see trace A of Figure 2). This preference is based on the reasonable assumption of similar band contours for  $\nu_5$  in  $\text{HNF}_2$  and  $\text{DNF}_2$ . Similarly, the band center of  $\nu_3(a')$  of  $\text{DNF}_2$  is preferably assigned to 962  $\text{cm}^{-1}$  instead of the previously proposed<sup>9</sup> value of 972  $\text{cm}^{-1}$ . The 962- $\text{cm}^{-1}$  value is also supported by the observation of the  $(\nu_3 + \nu_6)(a'')$  combination band at 1849  $\text{cm}^{-1}$  (calculated for 962 + 888 = 1850  $\text{cm}^{-1}$ ). It is also noteworthy that our revised frequency values for  $\text{DNF}_2$  result in a better match with those obtained by Pulay and co-workers by ab initio calculations from the  $\text{HNF}_2$  values.<sup>17</sup>

The liquid-phase frequencies are almost identical with the gas-phase values (see Table I), indicating only weak association for liquid difluoramine. The only remarkable feature is the

(17) Fogarasi, G.; Pulay, P.; Molt, K.; Sawodny, W. *Mol. Phys.* 1977, 33, 1565.

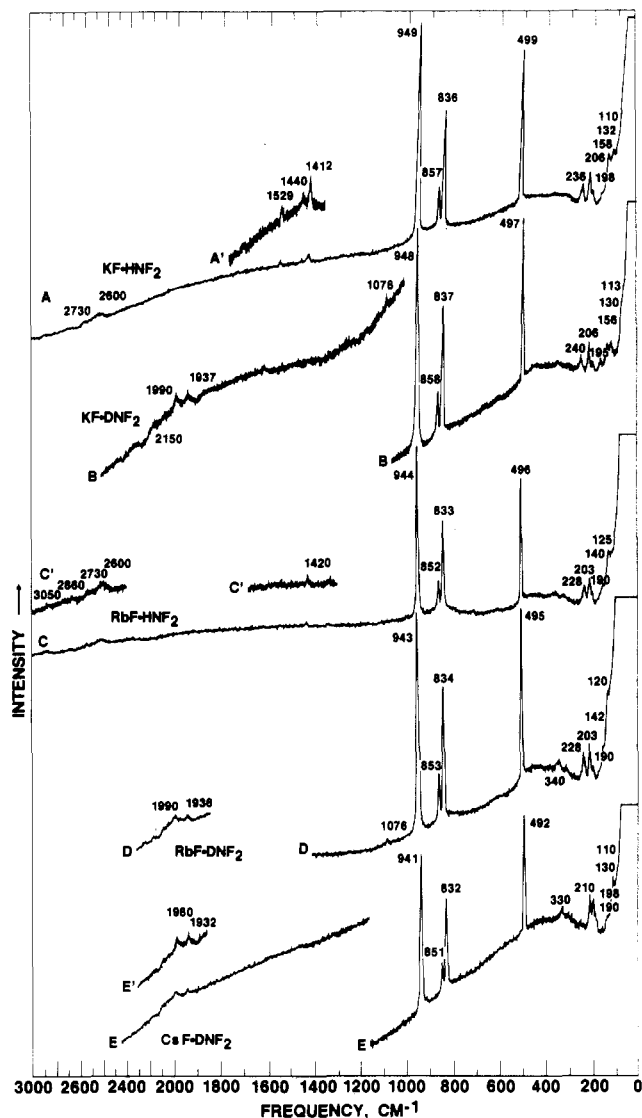


**Figure 4.** Raman spectra of  $\text{KF}\cdot\text{HNF}_2$  (traces A, A'),  $\text{KF}\cdot\text{DNF}_2$  (trace B),  $\text{RbF}\cdot\text{HNF}_2$  (traces C and C'),  $\text{RbF}\cdot\text{DNF}_2$  (trace D), and  $\text{CsF}\cdot\text{DNF}_2$  (traces E and E'), all recorded at  $-140^\circ\text{C}$ . Traces A', C', and E' were recorded at a higher sensitivity setting.

splitting of the NH and the ND stretching mode,  $\nu_1(a')$ , into two components. These splittings and their relative Raman intensities and polarization ratios are similar for both  $\text{HNF}_2$  and  $\text{DNF}_2$  and do not permit their attribution to combination bands in Fermi resonance with  $\nu_1$ . Similar splittings have been observed for the symmetric stretching modes of liquid  $\text{NH}_3$  and  $\text{ND}_3$ <sup>18</sup> and solid  $\text{HOF}$ <sup>19</sup> and have been attributed to aggregates.<sup>19,20</sup> Therefore, this explanation is also preferred for difluoramine.

For solid difluoramine the previously reported infrared spectrum had been recorded with only low precision in the  $\text{NaCl}$  region<sup>10</sup> and deviates significantly from that given in Figure 3. Compared to the liquid-phase values, the NH stretching frequency of solid  $\text{HNF}_2$  decreased by about  $40\text{ cm}^{-1}$  and the NH deformation frequencies increased by about  $23\text{ cm}^{-1}$ . Furthermore, all these modes are split into two components each, and bands due to libration and lattice modes appear below  $310\text{ cm}^{-1}$ . All these features suggest an increased degree of association. Since the N-H modes are shifted and split relative to the gas phase, and those of the  $\text{NF}_2$  group are not, the association must involve intermolecular N-H...N and not N-H...F bridges. This surprising result is discussed elsewhere in more detail.<sup>21</sup> The fact that in  $\text{HNF}_2$

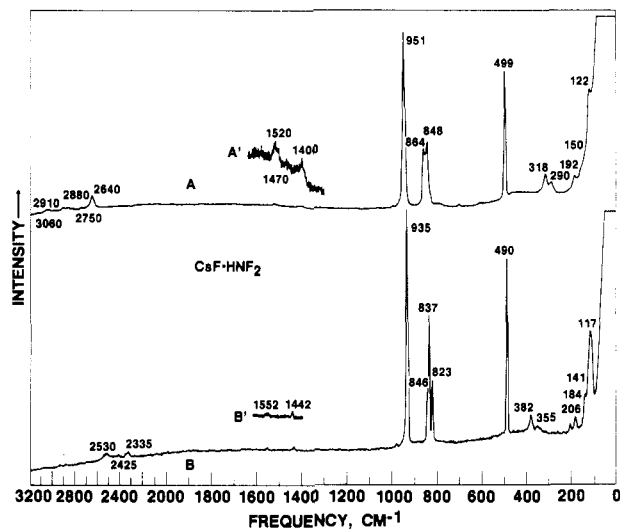
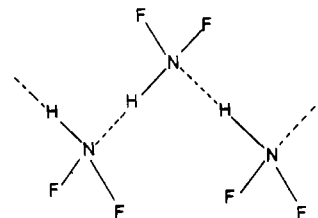


**Figure 5.** Raman spectra of the two modifications of  $\text{CsF}\cdot\text{HNF}_2$  at  $-140^\circ\text{C}$ . Traces A and A' show the spectrum of the more weakly hydrogen-bridged adduct at two different sensitivity levels, respectively, and traces B and B' show those of the stronger hydrogen-bridged adduct.

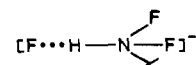
the nitrogen is a better electron donor than fluorine is in accord with the previous report by Craig that the weak  $\text{HNF}_2\cdot\text{BF}_3$  and  $\text{HNF}_2\cdot\text{BCl}_3$  donor-acceptor adducts contain B-N and not B-F bridges.<sup>10</sup> By analogy with the known structure of solid  $\text{HF}$ ,<sup>21</sup> a zigzag chain structure, such as



is most likely for  $(\text{HNF}_2)_n$ , but without additional structural support a more detailed interpretation of the vibrational data appears unwarranted.

**Vibrational Spectra and Structure of the  $\text{MF}\cdot\text{HNF}_2$  Adducts.** Adducts of both  $\text{HNF}_2$  and  $\text{DNF}_2$  with  $\text{KF}$ ,  $\text{RbF}$ , and  $\text{CsF}$  were prepared as previously described.<sup>6</sup> When an excess of unreacted  $\text{HNF}_2$  was used in the syntheses, followed by removal of unreacted  $\text{HNF}_2$  at low temperature, the combining ratios approximated 1:1. Low-temperature Raman spectra were measured for all these adducts (Figures 4 and 5). Low-temperature infrared spectra were recorded only for  $\text{RbF}\cdot\text{HNF}_2$  (Figure 3) due to the limited availability of the corresponding alkali-metal fluoride windows and the treacherous explosiveness of the  $\text{CsF}\cdot\text{HNF}_2$  adduct on warm-up to ambient temperature, which caused severe damage to the cryostats.

The Raman spectra of  $\text{MF}\cdot\text{HNF}_2$  ( $\text{M} = \text{K}$  and  $\text{Rb}$ ) and  $\text{MF}\cdot\text{DNF}_2$  ( $\text{M} = \text{K}$ ,  $\text{Rb}$ , and  $\text{Cs}$ ) were completely analogous (see Figure 3 and Table II), suggesting essentially identical structures for these adducts. Compared to the spectra of free  $\text{HNF}_2$  (see above), the frequency of the N-H stretching mode has decreased by about  $600\text{ cm}^{-1}$  and consists of numerous broad bands. The two N-H deformation frequencies have increased by about  $100\text{ cm}^{-1}$  and are also split, whereas the three  $\text{NF}_2$  modes exhibit only relatively small frequency decreases with  $\nu_{\text{as}}(\text{NF}_2)$  also being split. These observations are thoroughly consistent with an adduct involving a strong hydrogen bridge between  $\text{HNF}_2$  and the fluoride anion



(18) De Bettignies, B.; Wallart, F. C. R. *Seances Acad. Sci., Ser. B* **1972**, 275, 283.

(19) Kim, H.; Appelman, E. H. *J. Chem. Phys.* **1982**, 76, 1664.

(20) Abouaf-Marguin, L.; Jacox, M. E.; Milligan, D. E. *J. Mol. Spectrosc.* **1977**, 67, 34.

(21) Christe, K. O. *J. Fluorine Chem.*, in press.

(22) Atoji, M.; Lipscomb, W. N. *Acta Crystallogr.* **1954**, 7, 173.

Table I. Vibrational Spectra of HNF<sub>2</sub> and DNF<sub>2</sub> in the Gas, Liquid, and Solid Phases

| assignt                               | approx<br>descrip of<br>mode        | obsd freq, cm <sup>-1</sup> (rel intens <sup>a</sup> ) |                 |         |            |                     |                 |                |                           |            |
|---------------------------------------|-------------------------------------|--------------------------------------------------------|-----------------|---------|------------|---------------------|-----------------|----------------|---------------------------|------------|
|                                       |                                     | HNF <sub>2</sub>                                       |                 |         |            | DNF <sub>2</sub>    |                 |                |                           |            |
|                                       |                                     | gas<br>IR                                              | liquid<br>Raman | solid   |            | gas<br>IR           | liquid<br>Raman | solid<br>Raman | gas<br>calcd <sup>b</sup> |            |
| C <sub>s</sub>                        |                                     |                                                        |                 |         |            |                     |                 |                |                           |            |
| ν <sub>1</sub> (a')                   | ν(NH)                               | 3193 vw                                                | 3210 (0.8) p    | 3215 w  | 3163 (0.8) | [2333] <sup>c</sup> | 2388 (1) p      | 2353 (3.2)     | 2340                      |            |
|                                       |                                     |                                                        | 3185 (1.7) p    | 3170 sh | 3139 (2.0) |                     |                 | 2365 (2.2) p   |                           | 2338 (10)  |
|                                       |                                     |                                                        |                 | 3158 s  | 2874 mw    |                     |                 |                |                           | 2107 (0+)  |
|                                       |                                     |                                                        |                 | 2730 vw | 2650 mw    |                     |                 |                |                           |            |
| 2ν <sub>3</sub> (a')                  |                                     |                                                        |                 | 2340 w  |            |                     |                 |                |                           |            |
| ν <sub>2</sub> + ν <sub>5</sub> (a'') |                                     |                                                        |                 |         |            |                     |                 |                |                           |            |
| 2ν <sub>2</sub> (a')                  |                                     |                                                        |                 | 2650 mw |            |                     |                 |                |                           |            |
| ν <sub>5</sub> + ν <sub>6</sub> (a')  |                                     |                                                        |                 | 2340 w  |            |                     |                 |                |                           |            |
| ν <sub>2</sub> + ν <sub>6</sub> (a'') |                                     |                                                        |                 |         |            |                     | 1897 vw         |                |                           |            |
| ν <sub>3</sub> + ν <sub>6</sub> (a'') |                                     | 1850 mw                                                |                 | 1850 sh |            |                     | 1849 mw         |                |                           |            |
| ν <sub>2</sub> + ν <sub>4</sub> (a')  |                                     |                                                        |                 | 1825 mw |            |                     |                 |                |                           |            |
| ν <sub>5</sub> (a'')                  | δ <sub>as</sub> (F <sub>2</sub> NH) | 1424 s                                                 | 1429 (0.9) dp   | 1460 sh | 1462 (0.3) | 1028 s              | 1043 (0.8) dp   | 1070 (0.6)     | 1034                      |            |
|                                       |                                     |                                                        |                 | 1445 s  | 1446 (0.3) |                     |                 |                |                           | 1059 (0.6) |
|                                       |                                     |                                                        | 1426 s          | 1343 s  | 1360 (0.1) |                     |                 | 1036 (0.5)     |                           |            |
| ν <sub>2</sub> (a')                   | δ <sub>s</sub> (F <sub>2</sub> NH)  | 1307 s                                                 | 1310 (0.7) p    | 1310 s  | 1304 (0.5) | 1009 s              | 1007 (2) p      | 1003 (1.2)     | 1007                      |            |
|                                       |                                     |                                                        |                 | 1008 sh | 1006 m     |                     |                 | 1110 (0+)      |                           |            |
| 2ν <sub>4</sub> (a')                  |                                     |                                                        |                 | 967 s   | 978 (10)   |                     |                 | 977 (10)       | 961                       |            |
| ν <sub>3</sub> (a')                   | ν <sub>s</sub> (NF <sub>2</sub> )   | 972 ms                                                 | 974 (10) p      | 967 s   | 978 (10)   | 962 ms              | 970 (10) p      | 977 (10)       | 961                       |            |
| ν <sub>6</sub> (a'')                  | ν <sub>as</sub> (NF <sub>2</sub> )  | 888 vs                                                 | 869 (4.0) dp    | 875 vs  | 868 (7.3)  | 888 vs              | 866 (3.6) dp    | 868 (8.3)      | 888                       |            |
|                                       |                                     |                                                        |                 | 735 mw  |            |                     |                 |                |                           |            |
| ν <sub>4</sub> (a')                   | δ <sub>s</sub> (NF <sub>2</sub> )   | 500 mw                                                 | 504 (8.2) p     | 503 m   | 505 (5.4)  | 498 mw              | 501 (8.4) p     | 503 (5.2)      | 498                       |            |
|                                       |                                     |                                                        |                 |         | 305 (0.7)  |                     |                 | 284 (1.0)      |                           |            |
|                                       |                                     |                                                        |                 |         | 149 (0.3)  |                     |                 | 144 (1)        |                           |            |
|                                       |                                     |                                                        |                 |         |            |                     |                 | 114 (3)        |                           |            |
|                                       |                                     |                                                        |                 |         |            |                     |                 | 103 (3)        |                           |            |
|                                       |                                     |                                                        |                 |         |            |                     |                 | 75 (2)         |                           |            |

<sup>a</sup>Uncorrected Raman intensities (peak heights). <sup>b</sup>Data from ref 17, calculated by ab initio methods from HNF<sub>2</sub> values. <sup>c</sup>Estimated value from ref 9; not observed in this study because of its low intensity.

Table II. Vibrational Spectra of the Alkali-Metal Fluoride-Difluoramine Adducts<sup>a</sup>

| assignt for<br>[F...H-NF <sub>2</sub> ] <sup>-c</sup> | obsd freq, cm <sup>-1</sup> (rel intens <sup>b</sup> ) |                              |                      |         |                               |                      |            |                               |            |
|-------------------------------------------------------|--------------------------------------------------------|------------------------------|----------------------|---------|-------------------------------|----------------------|------------|-------------------------------|------------|
|                                                       | KF·HNF <sub>2</sub><br>Raman                           | KF·DNF <sub>2</sub><br>Raman | RbF·HNF <sub>2</sub> |         | RbF·DNF <sub>2</sub><br>Raman | CsF·HNF <sub>2</sub> |            | CsF·DNF <sub>2</sub><br>Raman |            |
|                                                       |                                                        |                              | Raman                | IR(I)   | IR(II)                        |                      | Raman (I)  | Raman (II)                    |            |
| ν(N-H)(I)                                             | 2730 (0.1)                                             | 2160 (0.3)                   | 3050 (0.1)           | 3050 mw |                               | 2160 (0+)            | 3060 (0.2) |                               |            |
|                                                       |                                                        | 2080 (0.1)                   |                      | 2870 m  |                               | 2085 (0+)            | 2910 (0.2) |                               | 2080 (0+)  |
|                                                       |                                                        | 2040 (0+)                    | 2860 (0.1)           | 2870 m  |                               | 2035 (0+)            | 2880 (0.2) |                               | 2035 (0+)  |
|                                                       |                                                        | 1990 (0.6)                   | 2730 (0.1)           | 2658 s  |                               | 1990 (0.5)           | 2750 (0.1) |                               | 1980 (0.3) |
| 2600 (0.3)                                            | 1937 (0.5)                                             | 2600 (0.3)                   |                      |         | 1936 (0.2)                    | 2640 (0.6)           |            | 1932 (0.2)                    |            |
| ν(N-H)(II)                                            |                                                        |                              |                      | 2540 sh |                               |                      | 2530 (0.3) |                               |            |
|                                                       |                                                        |                              |                      | 2430 m  |                               |                      | 2425 (0.1) |                               |            |
|                                                       |                                                        |                              |                      | 2325 m  |                               |                      | 2335 (0.2) |                               |            |
|                                                       |                                                        |                              |                      | 1553 mw |                               |                      | 1552 (0.1) |                               |            |
| δ <sub>as</sub> (HNF <sub>2</sub> )(II)               |                                                        |                              |                      |         |                               |                      |            |                               |            |
| δ <sub>as</sub> (HNF <sub>2</sub> )(I)                | 1529 (0.2)                                             |                              |                      | 1506 mw |                               |                      | 1520 (0.1) |                               |            |
| δ <sub>s</sub> (HNF <sub>2</sub> )(II)                |                                                        |                              |                      |         | 1474 w                        |                      |            |                               |            |
|                                                       |                                                        |                              |                      |         | 1439 m                        |                      |            | 1442 (0.1)                    |            |
|                                                       | 1440 (0.1)                                             |                              |                      |         |                               |                      |            |                               |            |
| δ <sub>s</sub> (HNF <sub>2</sub> )(I)                 | 1412 (0.4)                                             | 1076 (0.4)                   | 1420 (0.2)           | 1420 mw |                               | 1076 (0.2)           | 1470 (0+)  |                               |            |
| ν <sub>s</sub> (NF <sub>2</sub> )(I)                  | 949 (10)                                               | 948 (10)                     | 944 (10)             | 942 s   |                               | 943 (10)             | 951 (10)   |                               | 941 (10)   |
| ν <sub>s</sub> (NF <sub>2</sub> )(II)                 |                                                        |                              |                      |         | 930 s                         |                      |            | 935 (10)                      |            |
| ν <sub>as</sub> (NF <sub>2</sub> )(I)                 | 857 (1.7)                                              | 858 (1.7)                    | 852 (1.7)            | 849 sh  |                               | 853 (2)              | 864 (3)    |                               | 851 (1.5)  |
|                                                       | 836 (5.5)                                              | 837 (5.5)                    | 833 (5.5)            | 831 vs  |                               | 834 (5.7)            | 848 (3.5)  |                               | 832 (5.5)  |
| ν <sub>as</sub> (NF <sub>2</sub> )(II)                |                                                        |                              |                      |         | 838 vs                        |                      |            | 846 sh                        |            |
|                                                       |                                                        |                              |                      |         | 821 sh                        |                      |            | 837 (5.2)                     |            |
|                                                       |                                                        |                              |                      |         |                               |                      |            | 823 (2.5)                     |            |
| δ <sub>s</sub> (NF <sub>2</sub> )(I)                  | 499 (7.1)                                              | 497 (7.2)                    | 496 (7.2)            | 498 mw  |                               | 495 (7.5)            | 499 (7.1)  |                               | 492 (7.5)  |
| δ <sub>s</sub> (NF <sub>2</sub> )(II)                 |                                                        |                              |                      |         | 490 mw                        |                      |            | 490 (7)                       |            |
|                                                       |                                                        |                              | 350 (0.1)            | 330 vs  |                               | 340 (0.3)            | 318 (1.0)  | 382 (0.7)                     | 330 (0.5)  |
|                                                       |                                                        |                              |                      |         |                               |                      | 290 (0.5)  | 355 (0.2)                     |            |
|                                                       | 236 (0.8)                                              | 240 (0.6)                    | 228 (0.6)            |         |                               | 228 (1)              | 192 (0.3)  | 206 (0.3)                     | 210 (2)    |
|                                                       | 206 (1.5)                                              | 206 (1)                      | 203 (1.2)            |         |                               | 203 (1.4)            | 150 sh     | 184 (0.5)                     | 198 (2)    |
|                                                       | 198 sh                                                 | 195 sh                       | 190 sh               |         |                               | 190 (0.4)            |            | 141 (0.2)                     | 190 sh     |
|                                                       | 158 sh                                                 | 156 (0.3)                    | 140 sh               |         |                               | 142 sh               |            |                               |            |
|                                                       | 132 (1)                                                | 130 (1)                      | 125 (1)              |         |                               | 120 sh               | 122 (1)    | 117 (3)                       | 130 sh     |
|                                                       | 110 (1)                                                | 113 (1)                      |                      |         |                               |                      |            |                               | 110 (1)    |
|                                                       |                                                        | 60 sh                        |                      |         |                               |                      |            |                               |            |

<sup>a</sup>I and II refer to the two modifications (see text for explanation). All Raman spectra were recorded at -140 °C; infrared spectra, at -220 °C. <sup>b</sup>Uncorrected Raman intensities (peak heights). <sup>c</sup>For the MF·DNF<sub>2</sub> adducts, assignments involving the N-D group have been listed in the N-H rows.

similar to those previously reported for  $\text{CsF}\cdot\text{HONO}_2^{23}$  and  $\text{KF}\cdot(\text{CH}_2\text{COOH})_2^{24}$ . The minor frequency decrease of the  $\text{NF}_2$  vibrations can be explained by the electron-density release from  $\text{F}^-$  to  $\text{HNF}_2$ , which increases the partial negative charges on the two fluorines of the  $\text{NF}_2$  group, causing an increase of the  $\text{NH}^{\delta+}\text{-F}^{\delta-}$  bond polarity and a decrease of the N-F force constants.

The Raman spectra of the corresponding  $\text{DNF}_2$  adducts are completely analogous and show the expected N-H:N-D frequency ratio of about 1.35–1.40. In addition to these major effects, all the spectra exhibit some more subtle features. For example, the  $\text{NF}_2$  modes show a frequency decrease of about  $10\text{ cm}^{-1}$  on going from  $\text{KF}\cdot\text{HNF}_2$  to  $\text{CsF}\cdot\text{HNF}_2$ . This can be ascribed to the higher negative charge on  $\text{F}^-$  in  $\text{CsF}$ , relative to that in  $\text{KF}$ .

In addition to the internal modes of the  $\text{HNF}_2$  subunit in the  $[\text{F}\cdots\text{H}\text{-NF}_2]^-$  anion, we would also expect librational modes due to the  $\text{F}\cdots\text{H}\text{-N}$  bridge, i.e. one  $\text{F}\cdots\text{H}$  stretch and two  $\text{F}\cdots\text{H}\text{-N}$  deformation modes. Furthermore, bands due to the interaction between the alkali-metal cations and the fluoride anions should be observable. All these modes should occur at relatively low frequencies and indeed numerous bands below  $350\text{ cm}^{-1}$  were observed. By analogy with the N-H modes, the  $\text{F}\cdots\text{H}$  modes are probably broad and of low Raman intensity and therefore difficult to observe in the Raman spectra. In the infrared spectra of  $\text{RbF}\cdot\text{HNF}_2$  (traces C and D of Figure 3) there is clear evidence for a strong absorption at about  $330\text{ cm}^{-1}$ , and this could be one of the  $\text{F}\cdots\text{H}$  libration modes. The sharper features observed in the  $240\text{-}190\text{-cm}^{-1}$  region of the Raman spectra do not exhibit the large deuterium isotopic shifts expected for the  $\text{F}\cdots\text{H}\text{-N}$  bridge modes and therefore are probably due to modes involving mainly fluoride ion motions in the lattice.

The Raman spectra of  $\text{CsF}\cdot\text{HNF}_2$  showed the following interesting additional features. Two different sets of bands were observed, which exhibited similar overall patterns but pronounced frequency shifts from each other, as shown by traces A and B of Figure 5. The spectrum depicted as trace A is very similar, although not quite analogous, to those of all the adducts given in Figure 4. The spectrum of trace B shows very pronounced frequency shifts (decrease of  $\nu(\text{NH})$  by about  $300\text{ cm}^{-1}$ , increase of the N-H deformations by about  $40\text{ cm}^{-1}$ , decrease of the  $\text{NF}_2$  modes by about  $10\text{-}30\text{ cm}^{-1}$ , and increase of the librational frequencies) relative to trace A. These shifts are best attributed to a hydrogen-bonded  $[\text{F}\cdots\text{HNF}_2]^-$  adduct, which is very similar to that discussed above for the other adducts but contains a significantly stronger hydrogen bridge. No evidence was observed for the existence of adducts showing frequencies intermediate between those of traces A and B, thus suggesting the presence of two distinct structures and not a progressive variation of the hydrogen-bond strength.

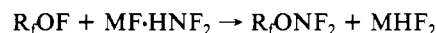
In the case of HF addition to the fluoride anion, each free valence electron pair of the fluoride can form a hydrogen bridge, resulting in the  $[\text{F}(\cdots\text{HF})_\eta]^-$  polyanions where  $\eta$  can range from 1 to 4.<sup>25-28</sup> The interpretation of the second, more strongly hydrogen-bridged  $\text{F}\cdots\text{HNF}_2$  type adduct in terms of an analogous  $[\text{F}(\cdots\text{HNF}_2)_\eta]^-$  anion can be ruled out because the observed frequency changes (decrease of the N-H and  $\text{NF}_2$  stretching modes) are opposite to those predicted for these polyanions.

Further evidence for the existence of a second, distinct, more strongly hydrogen-bonded adduct was obtained from the low-temperature infrared spectra of  $\text{RbF}\cdot\text{HNF}_2$  (see below). This demonstrates that the occurrence of a second, more strongly bridged  $\text{HNF}_2$  adduct is not limited to  $\text{CsF}$  but also occurs for  $\text{RbF}$ .

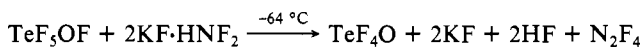
For the low-temperature infrared spectra of  $\text{RbF}\cdot\text{HNF}_2$ , di-fluoramine was condensed at  $-220\text{ }^\circ\text{C}$  onto an  $\text{RbF}$  single-crystal window. After the spectrum of the solid  $\text{HNF}_2$  deposit was recorded (Figure 3, trace B), the temperature of the  $\text{RbF}$  window was warmed briefly to  $-110\text{ }^\circ\text{C}$  in a static vacuum. Volatile material was pumped off quickly at  $-110\text{ }^\circ\text{C}$ , and the window was cooled back again to  $-220\text{ }^\circ\text{C}$ . The infrared spectrum of the resulting product (Figure 3, trace C) showed the absence of any unreacted  $\text{HNF}_2$  and corresponded well to the low-temperature Raman spectra of the  $\text{MF}\cdot\text{HNF}_2$  adducts shown in Figure 4. When the temperature of the infrared sample was briefly cycled through  $-105\text{ }^\circ\text{C}$  and cooled down again to  $-220\text{ }^\circ\text{C}$ , additional bands were observed, which are marked in trace D of Figure 3 by a dagger. The frequencies of these bands are almost identical with those of the major Raman bands of the more strongly hydrogen-bonded modification of the  $\text{CsF}\cdot\text{HNF}_2$  adduct shown in trace B of Figure 5 and were assigned accordingly (see Table II). Cycling of the  $\text{RbF}\cdot\text{HNF}_2$  sample from  $-220\text{ }^\circ\text{C}$  through ambient temperature in a dynamic vacuum resulted in the disappearance of the bands attributed to these  $\text{RbF}\cdot\text{HNF}_2$  adducts.

Comparison of the results from this work with those from a previous low-temperature infrared study<sup>6</sup> show only fair to poor agreement. This disagreement can be attributed to the poor quality of the previously reported data, which is no surprise in view of the great experimental difficulties encountered. Although the existence of two different types of compounds, one a hydrogen-bonded  $\text{MF}\cdots\text{HNF}_2$  compound and the other an  $\text{MNF}_2\cdot\text{HF}$  adduct, had been postulated, this conclusion was based more on the then known reaction chemistry of the adducts than on the spectroscopic data. The  $\text{MNF}_2\cdot\text{HF}$  structure had been proposed to account for the fact that only  $\text{CsF}\cdot\text{HNF}_2$  exhibited a propensity to explode on warming toward room temperature. The present study demonstrates that the  $\text{KF}\cdot\text{HNF}_2$ ,  $\text{RbF}\cdot\text{HNF}_2$ , and  $\text{CsF}\cdot\text{HNF}_2$  adducts exhibit the same structural features involving a strong hydrogen bridge between the  $\text{HNF}_2$  and the fluoride anion of the alkali-metal fluoride, and that the existence of a second, distinct modification which differs from the first one only in the strength of its hydrogen bridge is not unique for  $\text{CsF}$ . Although this second modification appears to form more readily with  $\text{CsF}$ , it was also observed for  $\text{RbF}$  and therefore might not necessarily be the main reason for the explosive nature of  $\text{CsF}\cdot\text{HNF}_2$ . Other factors, such as the higher affinity of  $\text{CsF}$  for HF, might be significant contributors. No evidence was obtained in this study for the presence of a distinct  $\text{NF}_2^-$  anion, which should exhibit vibrational spectra very different from those observed.<sup>29</sup>

**Reaction Chemistry of  $\text{MF}\cdot\text{HNF}_2$  Adducts.** Since  $\text{MF}\cdot\text{HNF}_2$  adducts are known to react with perfluoroalkyl hypofluorites according to



the analogous reactions were studied for several hypofluorites for which the corresponding  $-\text{ONF}_2$  derivatives are still unknown. The hypofluorites studied included  $\text{TeF}_3\text{OF}$ ,  $\text{FOClO}_3$ , and  $\text{FONO}_2$ . In the case of  $\text{TeF}_3\text{OF}$  the observed reaction products are best explained by the oxidation of  $\text{HNF}_2$  by  $\text{TeF}_3\text{OF}$



followed by the competing reactions



The reaction of  $\text{OF}_2$  with  $\text{KF}\cdot\text{HNF}_2$  required a considerably higher temperature and even at  $-22\text{ }^\circ\text{C}$  was still incomplete after 1 h.

(23) Al-Zamil, A.; Delf, B. W.; Gillard, R. D. *J. Inorg. Nucl. Chem.* **1980**, *42*, 1117.

(24) Jones, D. J.; Emsley, J.; Roziere, J. *J. Chem. Soc., Dalton Trans.* **1984**, 1625.

(25) Coyle, B. A.; Schroeder, L. W.; Ibers, J. A. *J. Solid State Chem.* **1970**, *1*, 386.

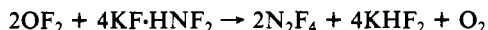
(26) Gennick, I.; Harmon, K. M.; Potvin, M. M. *Inorg. Chem.* **1977**, *16*, 2033.

(27) Harmon, K. M.; Gennick, I. *J. Mol. Spectrosc.* **1977**, *38*, 97.

(28) Mootz, D.; Poll, W. *Z. Naturforsch., B: Anorg. Chem., Org. Chem.* **1984**, *39B*, 1300.

(29) **Note Added in Proof.** Since submission of this paper, warm-up of  $\text{RbF}\cdot\text{HNF}_2$  has also resulted in some instances in explosions.

Again the main reaction was the oxidation of  $\text{HNF}_2$  to  $\text{N}_2\text{F}_4$ .



In the case of  $\text{FOClO}_3$  and  $\text{KF}\cdot\text{HNF}_2$ , the mixture exploded when warmed from  $-196$  toward  $-78$  °C. For  $\text{FONO}_2$ , the reaction could be sufficiently controlled, but again  $\text{N}_2\text{F}_4$  was formed in almost quantitative yield with  $\text{NO}_2$ ,  $\text{O}_2$ , and  $\text{FNO}_2$  as the major byproducts. It thus appears that with hypofluorites, which are powerful oxidizers, fluorination of  $\text{HNF}_2$  to  $\text{N}_2\text{F}_4$  and HF is

favored over  $\text{XONF}_2$  formation.

**Acknowledgment.** The authors are grateful to Drs. C. J. Schack, W. W. Wilson, and L. R. Grant for their help and to the Army Research Office and the Office of Naval Research for financial support.

**Registry No.**  $\text{D}_2$ , 7782-39-0;  $\text{HNF}_2$ , 10405-27-3;  $\text{KF}$ , 7789-23-3;  $\text{RbF}$ , 13446-74-7;  $\text{CsF}$ , 13400-13-0;  $\text{TeF}_2\text{OF}$ , 83314-21-0;  $\text{OF}_2$ , 7783-41-7;  $\text{FONO}_2$ , 7789-26-6;  $\text{FOClO}_3$ , 10049-03-3;  $\text{HF}$ , 7664-39-3;  $\text{N}_2\text{F}_4$ , 10036-47-2.

Contribution from the Max-Planck-Institut für Biophysikalische Chemie, 34 Göttingen-Nikolausberg, West Germany

## Kinetics of the Consecutive Binding of Bipyridyl Ligands and of Phenanthroline Ligands to Copper(II)

I. Fábrián<sup>1</sup> and H. Diebler\*

Received July 30, 1986

By the application of temperature-jump relaxation techniques, the kinetics of the consecutive binding of bipyridyl ligands (bpy) and of phenanthroline ligands (phen) to Cu(II) have been studied,  $\text{CuL}_{i-1}^{2+} + \text{L} \xrightarrow{k_i} \text{CuL}_i^{2+}$  ( $i = 2, 3$ ;  $\text{L} = \text{bpy, phen}$ ). At 25 °C and ionic strength 0.5 M, the following forward rate constants have been obtained: for bpy,  $k_2 = 1.5 \times 10^9 \text{ M}^{-1} \text{ s}^{-1}$  and  $k_3 = 8.6 \times 10^8 \text{ M}^{-1} \text{ s}^{-1}$ ; for phen,  $k_2 = 6.9 \times 10^8 \text{ M}^{-1} \text{ s}^{-1}$  and  $k_3 = 1.8 \times 10^9 \text{ M}^{-1} \text{ s}^{-1}$ . These rate constants are appreciably larger than those for formation of the 1:1 complexes, which were determined earlier,  $k_1 = (4-5) \times 10^7$  and  $6.4 \times 10^7 \text{ M}^{-1} \text{ s}^{-1}$ , respectively. The rate enhancement in the formation of the bis and tris complexes is attributed to stacking interactions between the coordinated and the incoming ligands. Several kinetic features of these reactions are discussed.

### Introduction

Complex formation processes involving Cu(II) are usually very fast, with second-order rate constants not far below the diffusion-controlled limit.<sup>2,3</sup> The rapidity of these reactions not only requires the application of specialized techniques for their investigation but also impedes the elucidation of mechanistic details. Several experimental studies have indicated that substitution processes at hexacoordinated Cu(II) are best described to proceed by a dissociative mechanism,<sup>3-5</sup> like those of various other divalent metal ions. On the other hand, associative mechanisms for Cu(II) have also been suggested.<sup>6,7</sup>

The high rates of substitution at  $\text{Cu}(\text{H}_2\text{O})_6^{2+}$  reflect the weak binding of the  $\text{H}_2\text{O}$  ligands in the axial positions of the distorted octahedron.<sup>8</sup> The observation that many multidentate ligands, too, react very fast with  $\text{Cu}^{2+}$  is obviously due to a rapid inversion of the Jahn-Teller distortion.<sup>3,8</sup> It has been reported that for  $\text{Cu}(\text{H}_2\text{O})_6^{2+}$  this inversion occurs with a rate of  $6 \times 10^{10} \text{ s}^{-1}$ .<sup>9</sup>

A subject of wide interest is the effects of ligands already coordinated to metal ions on the kinetics of further ligand binding.<sup>2</sup> A variety of factors may be of importance in this context: steric and electronic effects, inhibited Jahn-Teller inversion, and specific interactions between the ligands already bound and the incoming ligand. In this paper we report on the kinetics of the consecutive binding of 2,2'-bipyridyl (bpy) and of 1,10-phenanthroline (phen)

**Table I.** Values of  $\log K_{\text{stab}}$  for Complexes of bpy and phen (25 °C;  $I = 0.5 \text{ M}$ )

|                                                    |                | log K             |     |                   |     |
|----------------------------------------------------|----------------|-------------------|-----|-------------------|-----|
|                                                    |                | bpy               | ref | phen              | ref |
| $\text{H}^+ + \text{L} = \text{HL}^+$              | $K_{\text{H}}$ | 4.54              | 14  | 5.03              | 17  |
| $\text{Cu}^{2+} + \text{L} = \text{CuL}^{2+}$      | $K_1$          | 8.70 <sup>a</sup> | 10  | 9.20              | 17  |
| $\text{CuL}^{2+} + \text{L} = \text{CuL}_2^{2+}$   | $K_2$          | 5.78              | 15  | 6.70              | 17  |
|                                                    |                | 5.70 <sup>b</sup> |     | 6.69 <sup>b</sup> |     |
| $\text{CuL}_2^{2+} + \text{L} = \text{CuL}_3^{2+}$ | $K_3$          | 3.25 <sup>c</sup> | 16  | 5.20              | 17  |

<sup>a</sup> $I = 0.3 \text{ M}$ . <sup>b</sup>This work; see text. <sup>c</sup> $I = 1.0 \text{ M}$ .

to Cu(II) to form the corresponding bis and tris complexes,  $\text{CuL}_{i-1}^{2+} + \text{L} \rightleftharpoons \text{CuL}_i^{2+}$  ( $i = 2, 3$ ). The rates of formation of the 1:1 complex species have been previously determined.<sup>10,11</sup>

### Experimental Section

**Materials.** Stock solutions of  $\text{CuCl}_2$ , KCl, bpy, and phen were prepared from "reagent grade" chemicals (Merck) without further purification. In order to solubilize bpy and phen, equivalent amounts of HCl were added. The ligand solutions were kept in the dark to avoid any possible photodecomposition. The pH of the reactant solutions was brought to the desired value ( $\pm 0.01$ ) by the dropwise addition of 1 M KOH or HCl (Baker Chemicals). The ionic strength ( $I$ ) was adjusted to 0.5 M by using KCl. The chloride medium was chosen because of the UV absorption of  $\text{NO}_3^-$  and the solubility problems encountered in the presence of  $\text{ClO}_4^-$ .

**Methods.** pH measurements were carried out by means of a Radiometer PHM 52 digital pH meter equipped with a Metrohm EA 125 combined electrode. The calibration procedure for converting pH values to  $\text{H}^+$  concentrations was described elsewhere.<sup>4</sup> The kinetics of the complex formation reactions were studied by applying the temperature-jump relaxation technique with spectrophotometric detection.<sup>12</sup> The instrument used was either a conventional apparatus<sup>12</sup> with a lower limit of the accessible time range of 2  $\mu\text{s}$  or a cable T-jump apparatus<sup>13</sup> with

- (1) Permanent address: Institute of Inorganic and Analytical Chemistry, Kossuth-University, H-4010 Debrecen, Hungary.
- (2) Margerum, D. W.; Cayley, G. R.; Weatherburn, D. C.; Pagenkopf, G. K. In *Coordination Chemistry*; Martell, A. E., Ed.; American Chemical Society: Washington, DC, 1978; Vol. 2, p 1.
- (3) Wilkins, R. G. *The Study of Kinetics and Mechanism of Reactions of Transition Metal Complexes*; Allyn & Bacon: Boston, MA, 1974; pp 388-389.
- (4) Diebler, H.; Rosen, P. *Ber. Bunsen-Ges. Phys. Chem.* **1972**, *76*, 1031.
- (5) Moss, D. B.; Lin, C.; Rorabacher, D. B. *J. Am. Chem. Soc.* **1973**, *95*, 5179.
- (6) Sharma, V. S.; Leussing, D. L. *Inorg. Chem.* **1972**, *11*, 138.
- (7) Pasternack, R. F.; Huber, P. R.; Huber, U. M.; Sigel, H. *Inorg. Chem.* **1972**, *11*, 276.
- (8) Eigen, M. *Pure Appl. Chem.* **1963**, *6*, 97.
- (9) Poupko, R.; Luz, Z. *J. Chem. Phys.* **1972**, *57*, 3311.

- (10) Diebler, H. *Ber. Bunsen-Ges. Phys. Chem.* **1970**, *74*, 268.
- (11) Roche, T. S.; Wilkins, R. G. *J. Chem. Soc. D* **1970**, 1681.
- (12) Eigen, M.; De Maeyer, L. In *Technique of Organic Chemistry*, 2nd ed.; Weissberger, A., Ed.; Interscience: New York, 1963; Vol. VIII/2, p 895.